

Chapter 1

Phase-Space Methods for Fermions

Philippe Corboz

*School of Mathematics and Physics, The University of Queensland,
Brisbane, Queensland 4072, Australia*

Magnus Ögren, Karén Kheruntsyan and Joel F. Corney*

*ARC Centre of Excellence for Quantum-Atom Optics,
School of Mathematics and Physics, The University of Queensland,
Brisbane, Queensland 4072, Australia*

We review phase-space simulation techniques for fermions, showing how a Gaussian operator basis leads to exact calculations of the evolution of a many-body quantum system in both real and imaginary time. We give particular application to the Hubbard model and to the problem of molecular dissociation of bosonic molecules into pairs of fermionic atoms.

1.1. Introduction

Phase-space representations first arose from the attempt to describe quantum mechanics in terms of distributions over classical variables [1]. For example, Wigner introduced a function of phase-space variables $W(x, p)$ that would classically correspond to a joint-probability distribution: an integration over x gives the marginal distribution for p and vice-versa. However in quantum mechanics, such a function is not guaranteed to be positive; Wigner interpreted this feature as a quantum correction to classical statistical mechanics [2].

Besides providing insight into the quantum-classical correspondence, phase-space distributions lead to powerful calculation tools. Where they can be interpreted as true probability distributions, the phase-space functions can be sampled with stochastic trajectories, leading to efficient calculations of quantum dynamics or equilibrium states (see also Chapters ??, ??, ??, ?? ??).

*corney@physics.uq.edu.au

For bosonic systems, the well-known phase-space distributions — the Wigner, Husimi Q [3] and the Glauber-Sudarshan P functions [4, 5] — are based on coherent state expansions. So too are the related simulation techniques — the truncated Wigner method [6], and the exact $+P$ [7, 8] method — which have been widely used in quantum optics and ultracold atoms. For fermionic systems, coherent states do not play the same physical role. Although phase-space distributions using fermionic coherent states can be defined formally [9], they involve the use of anticommuting Grassmann numbers and do not have the same computational utility.

The underlying issue is that the superposition of a state containing an odd number of fermions with a state containing an even number of fermions is unphysical, due to the different transformation properties of states with integral and half-integral spin [10]. This superselection rule means that fermions can only be created in pairs. A much simpler, and yet complete, representation can therefore be achieved with a basis that involves superpositions of even numbers of fermions. Such a representation for bosons was developed earlier using squeezed states [11, 12]. Here we use a generalised Gaussian representation, which incorporates squeezed and thermal states for fermions into its basis.

The formalism and applications we present here are directed towards exact simulations of quantum evolution, for which we require a positive phase-space distribution that obeys a Fokker–Planck equation. This can be achieved with a basis that includes operators that do not just correspond to physical density matrices. Thus the distributions are defined over a domain of which only a subspace can be identified with the physical phase space (see also Chapter ??). This feature means that whereas *individual* stochastic trajectories cannot be identified with a particular physical history, the *ensemble average* does give the exact evolution of the quantum state. However, the restriction to a physical phase space or restrictions on the form of the distribution function [13] may lead to useful approximate methods.

1.2. Methodology

Most generally, a phase-space distribution is defined through an expansion of the density operator $\hat{\rho}$ over some (overcomplete) set of operators $\hat{\Lambda}$:

$$\hat{\rho} \equiv \sum_l P_l |\Psi\rangle \langle \Psi| = \int P(\alpha) \hat{\Lambda}(\alpha) d\alpha, \quad (1.1)$$

where α is the phase-space coordinate. By use of different sets of operators, different phase-space distributions can be constructed for the same quantum state. Any

observable quantity, which in quantum mechanics equates to the expectation value of an operator, can then be written as a moment of the phase-space distribution:

$$\langle \hat{A} \rangle \equiv \text{Tr}[\hat{A}\hat{\rho}] = \int P(\alpha)A(\alpha)d\alpha, \quad (1.2)$$

where $A(\alpha) \equiv \text{Tr}[\hat{A}\hat{\Lambda}(\alpha)]$ is the phase-space function corresponding to the observable.

To achieve a phase-space representation for fermions without using coherent states, we expand the density operator over a set of Gaussian operators. Mathematically, a Gaussian operator is an exponential of a quadratic form of annihilation and creation operators (see [14] for an explicit formation) and is characterised by its first-order moments:

$$\begin{aligned} \text{Tr}[\hat{c}_j\hat{c}_k\hat{\Lambda}] &= \Omega m_{jk}, & \text{Tr}[\hat{c}_j^\dagger\hat{c}_k\hat{\Lambda}] &= \Omega n_{jk}, \\ \text{Tr}[\hat{c}_k\hat{c}_j^\dagger\hat{\Lambda}] &= \Omega \bar{n}_{jk}, & \text{Tr}[\hat{c}_j^\dagger\hat{c}_k^\dagger\hat{\Lambda}] &= \Omega m_{jk}^+. \end{aligned} \quad (1.3)$$

where $\bar{n}_{jk} \equiv \delta_{jk} - n_{jk}$. Here $\Omega = \text{Tr}[\hat{\Lambda}]$ is a weighting factor, which is always positive for the applications given here. Higher-order, normally ordered correlations correspond to sums of products of these variables, according to a Wick factorisation.

In particular cases (where $\Omega = 1$, $m_{jk}^+ = m_{kj}^*$, $n_{jk} = n_{kj}^*$ and $0 \leq n_{jj} \leq 1$), the Gaussian operators are genuine density operators corresponding to certain physical states, such as squeezed and thermal states. In general, however, the operators are non-Hermitian, so that a positive distribution governed by a Fokker–Planck equation can always be obtained.

When used as a basis for a phase-space representation, the Gaussian operators map the evolution of $\hat{\rho}$ onto an ensemble of stochastic trajectories in the space of $\{\Omega, m_{jk}, m_{jk}^+, n_{jk}\}$. As indicated by Eq. (1.2), any expectation value can be calculated as the stochastic average of its corresponding phase-space function, for example, $\langle \hat{c}_j^\dagger\hat{c}_k \rangle_{\text{Quantum}} = \langle n_{jk} \rangle_{\text{Stochastic}}$, and

$$\langle \hat{c}_j^\dagger\hat{c}_k^\dagger\hat{c}_k\hat{c}_j \rangle_{\text{Quantum}} = \langle m_{jk}^+m_{kj} + n_{jj}n_{kk} - n_{jk}n_{kj} \rangle_{\text{Stochastic}}. \quad (1.4)$$

In general, one is interested in solving the equation $d\hat{\rho}/d\tau = \mathcal{L}[\hat{\rho}]$, where \mathcal{L} is a linear operator that gives either the Schrödinger picture time-evolution of the density operator, or the β -derivative of the grand-canonical ensemble density operator (in which case τ is the inverse temperature $\beta = 1/k_B T$). When these linear operators act on the elements of the basis $\hat{\Lambda}$ (as when the expansion Eq. (1.1) is used), they can be written in terms of derivatives with respect to phase-space variables [15]. By integrating by parts to transfer the derivatives onto P and assuming that boundary terms vanish, one obtains a Fokker–Planck equation that

can be sampled with stochastic trajectories, through the integration of an equivalent set of stochastic differential equations (SDEs). As applied to imaginary-time evolution, the approach is sometimes known as Gaussian Quantum Monte Carlo (GMC) or Gaussian-basis QMC.

Due to the overcompleteness of the Gaussian operators, the mapping to the distribution P is far from unique. This nonuniqueness allows a choice of possible stochastic realisations of the same quantum evolution. For quantum dynamics, for example, it allows the final stochastic equations to be tailored to reduce the fluctuations or improve the stability, and to thereby extend the useful simulation time [16]. For imaginary-time calculations, this choice allows the mapping to stable real equations with positive weights, enabling simulations down to very low temperatures [17].

1.2.1. Imaginary-Time Simulations: Hubbard Model

As an example we consider the 2d Hubbard model, which is a very simple model of strongly correlated electrons on a lattice [18], and which is believed to be relevant to cuprate high-temperature superconductors [19] (see also Chapters ??, ??, ??, which consider the Bose–Hubbard model). The Hamiltonian reads

$$\hat{H}_H - \mu\hat{N} = -J \sum_{\langle j,k \rangle, \sigma} (\hat{n}_{jk\sigma} + \text{H.c.}) + U \sum_j \hat{n}_{j\uparrow}\hat{n}_{j\downarrow} - \mu \sum_{j,\sigma} \hat{n}_{j\sigma}, \quad (1.5)$$

with $\hat{n}_{jk\sigma} = \hat{c}_{j\sigma}^\dagger \hat{c}_{k\sigma}$, where $\hat{c}_{j\sigma}^\dagger$ ($\hat{c}_{j\sigma}$) creates (annihilates) an electron with spin σ at the lattice site j . The parameter J is the hopping amplitude between nearest neighboring sites $\langle j, k \rangle$ on a square lattice, U is the on-site Coulomb interaction strength, and μ is the chemical potential to control the electron density. The generalisation to include, for example, an inhomogeneous trapping potential is straightforward.

To obtain a positive-definite diffusion matrix, we rewrite the interaction term in the Hamiltonian as

$$U \sum_j \hat{n}_{j\uparrow}\hat{n}_{j\downarrow} = -\frac{|U|}{2} \sum_j (n_{j\uparrow} - sn_{j\downarrow})^2 + \frac{|U|}{2} \sum_j (n_{j\uparrow} + n_{j\downarrow}), \quad (1.6)$$

where $s = \text{sign}(U)$ [14]. Applying the operator mappings from [14] leads to the following real Stratonovich SDEs in matrix form:

$$\frac{d\mathbf{n}_\sigma}{d\beta} = \frac{1}{2} (\bar{\mathbf{n}}_\sigma \mathbf{T}_\sigma^{(1)} \mathbf{n}_\sigma + \mathbf{n}_\sigma \mathbf{T}_\sigma^{(2)} \bar{\mathbf{n}}_\sigma), \quad (1.7)$$

$$T_{jk\sigma}^{(l)} = J\delta_{\langle j,k \rangle} + \delta_{jk} \left[|U| \left(n_{jj\sigma} - sn_{jj-\sigma} - \frac{1}{2} \right) + \mu + (\delta_{\sigma\uparrow} - s\delta_{\sigma\downarrow}) \xi_j^{(l)} \right], \quad (1.8)$$

with $\bar{\mathbf{n}}_\sigma = \mathbb{I} - \mathbf{n}_\sigma$, and $\xi_j^{(l)}(\beta)$ real Gaussian noise defined by the correlations

$$\langle \xi_j^{(l)}(\beta') \xi_j^{(l')}(\beta) \rangle = 2|U| \delta(\beta - \beta') \delta_{jj'} \delta_{ll'}. \quad (1.9)$$

As initial condition for the phase-space variables one chooses $n_{jk\sigma} = \delta_{jk}/2$, which represents the infinite-temperature density matrix. The initial weight of a trajectory can be chosen arbitrarily, and it evolves as

$$\frac{d\Omega(\beta)}{d\beta} = -\Omega H(\mathbf{n}), \quad (1.10)$$

with $H(\mathbf{n})$ being the Hamiltonian where operators have been replaced by their corresponding phase-space variables. Since all phase-space variables are real, the weight of a trajectory remains strictly positive. This enables an efficient Monte Carlo sampling without a sign problem by use of an appropriate importance sampling scheme, such as the Metropolis–Hastings algorithm [20] or a reconfiguration scheme of the trajectories as used in Green’s function Monte Carlo [21].

1.2.1.1. Symmetry Projection

In [22] it was observed that in some cases GMC fails to reproduce all symmetries of the Hamiltonian at low temperatures, which also results in a systematic deviation of the energy with respect to the true ground state energy. In the example of the Hubbard model, the $SU(2)$ spin rotation symmetry of the Hamiltonian is broken at very low temperatures, so that the low-temperature density matrix $\hat{\rho}$ has non-vanishing overlaps with the $S > 0$ spin sectors. These symmetries can be restored *a posteriori* by projecting $\hat{\rho}$ onto the symmetry sector of the ground-state,

$$\hat{\rho}_{Pr} = \hat{P} \hat{\rho} \hat{P}^\dagger, \quad (1.11)$$

where \hat{P} is the corresponding projection operator. Its form is given by group theory:

$$\hat{P}^\alpha = \frac{l_\alpha}{\sum_g} \sum_g \chi^\alpha(g)^\dagger \hat{T}(g), \quad (1.12)$$

where the sum^a goes over all elements g of the discrete^b symmetry group \mathcal{G} , and $\hat{T}(g)$ is the unitary operator corresponding to the group element g . l_α is the dimension of the α th irreducible representation \mathcal{D}^α of \mathcal{G} with character $\chi^\alpha(g)$, i.e. α selects the symmetry sector which the density matrix is projected onto. The operator $\hat{T}(g)$ maps the phase-space variables (Ω, \mathbf{n}) onto new variables $(\tilde{\Omega}, \tilde{\mathbf{n}})$,

^aThe sum in the denominator over all group elements yields the number of elements in the group.

^bIn the case of a continuous symmetry the sum \sum_g is replaced by an integral.

as explained in detail in [22]. Several projection operators can be combined, depending on the number of symmetries of the Hamiltonian, e.g. projection onto a specific total momentum sector (translational invariance), spin $S = 0$ [SU(2) symmetry], or particle number [U(1) symmetry].

1.2.2. Real-Time Dynamics

The application of the Gaussian method to real-time evolution gives the fermionic equivalent of the $+P$ method for bosons, which yields exact quantum dynamics for short times.

To show how the method works for systems with two-body interactions, we again focus on the fermionic Hubbard model [Eq. (1.5)], but with the possibility of an inhomogeneous trapping potential $V_{j\sigma}$. To succinctly represent the ‘mean field,’ or deterministic part of the resulting phase-space equations, we introduce matrices \mathbf{A}_σ with components

$$A_{jk\sigma} = -J\delta_{(j,k)} + \delta_{jk} (Un_{jj,-\sigma} + V_{j\sigma}). \quad (1.13)$$

The Itô SDEs can then be written

$$\begin{aligned} \dot{\mathbf{n}}_\uparrow &= -i(\mathbf{n}_\uparrow \mathbf{A}_\uparrow - \mathbf{A}_\uparrow \mathbf{n}_\uparrow) + \sqrt{-iU} \mathbf{n}_\uparrow \zeta^{(1)} \bar{\mathbf{n}}_\uparrow + \sqrt{iU} \bar{\mathbf{n}}_\uparrow \zeta^{(2)} \mathbf{n}_\uparrow, \\ \dot{\mathbf{n}}_\downarrow &= -i(\mathbf{n}_\downarrow \mathbf{A}_\downarrow - \mathbf{A}_\downarrow \mathbf{n}_\downarrow) + \sqrt{-iU} \mathbf{n}_\downarrow \zeta^{(1)*} \bar{\mathbf{n}}_\downarrow + \sqrt{iU} \bar{\mathbf{n}}_\downarrow \zeta^{(2)*} \mathbf{n}_\downarrow, \end{aligned} \quad (1.14)$$

where again $\bar{\mathbf{n}}_\sigma = \mathbb{I} - \mathbf{n}_\sigma$, and where $\zeta^{(l)}$ ($l = 1, 2$) are diagonal matrices of complex Gaussian noises, with correlations

$$\langle \zeta_{jj}^{(l)}(t) \zeta_{j'j'}^{(l')*}(t') \rangle = \delta(t - t') \delta_{jj'} \delta_{ll'}. \quad (1.15)$$

Neglecting the stochastic terms in Eq. (1.14) gives rise to the time-dependent Hartree–Fock approximation [13]. The noise terms thus give the quantum corrections to the mean-field approach.

Simulations of Eq. (1.14) for few-site systems show excellent agreement with the exact matrix calculations. Extension up to several hundred sites is numerically tractable. The practical weakness of the method so far is a limited simulation time in the case of strong interaction.

1.3. Applications

1.3.1. Application I: Ground-State of the Hubbard Model

The GMC method with and without symmetry projection was systematically tested in [22] for the 2d Hubbard model up to a lattice size 6×6 , and in [23]

for Hubbard ladders up to a size 16×2 , for different interaction strengths U/J and electron density. In the following we summarise the most important results.

For weakly interacting electrons, $U/J \leq 4$, GMC correctly reproduces quantities of interest, e.g. energies and correlation functions. Note that the magnitude of U enters as a prefactor in the diffusion term. Thus, if the diffusion term is small compared to the drift term, then GMC reproduces the exact results accurately. For larger interaction strengths, the GMC solution exhibits systematic errors in various quantities, and some of the symmetries in the Hamiltonian are broken. Using the projection technique the results can be improved considerably, as for example shown in Fig. 1.1. However, for strong interaction $U/J > 8$ (and systems with more than ≈ 30 sites), errors remain also after symmetry projection. One observes also that with increasing U/J and system size, the overlap of the simulated $\hat{\rho}$ with the ground state sector diminishes, i.e. it becomes more difficult to extract the ground state solution from $\hat{\rho}$. Thus, the projection scheme works well in the case where $\hat{\rho}$ has a large overlap with the true ground state with only a small admixture of excited states, which can be filtered out by the projection.

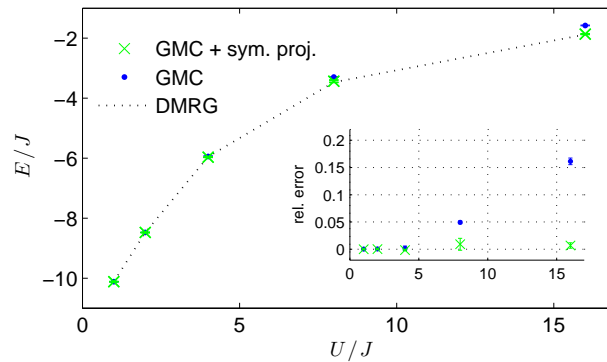


Fig. 1.1. Ground state energy in units of J of the half-filled 4×2 Hubbard ladder as a function of U/J . The inset shows the relative deviation with respect to the reference values, obtained by the density-matrix renormalisation group method (DMRG — see also Chapters ??, ??). Symmetry projection corrects the systematic deviations in the energy from the GMC simulation.

A variant of the symmetry projection scheme was proposed in [24], where the projection is included in the importance sampling. Instead of sampling trajectories according to their weight Ω , they are sampled with respect to their projected weights $\tilde{\Omega}$, which leads to a better convergence towards the ground state. One problem is that the projected weights can become negative (i.e. there is a sign problem), but this turns out to be tractable in most cases. This so-called pre-projection method was used to study pairing correlations in the doped 2d Hubbard

model up to a system size of 10×10 and $U/t = 7$. The analysis suggests that the pairing correlations are too weak to account for the superconductivity in the high-temperature cuprate superconductors (for dopings around $\delta \sim 0.2$), in contrast to the findings by some other methods (see e.g. [25–27]).

1.3.2. Application II: Dynamics of Molecular Dissociation

To date the real-time Gaussian phase-space method has mainly been applied to the problem of bosonic dimer molecules dissociating into pairs of free fermionic atoms of different spin [28] (see also Chapter ??, which considers molecule formation from bosonic atoms). The stochastic simulations reveal physics about the growth of correlations functions that cannot be obtained with the corresponding mean-field theory [29].

The Hamiltonian of this boson-fermion model [30] is

$$\hat{H} = \hbar \sum_{\mathbf{k}, \sigma} \Delta_{\mathbf{k}} \hat{n}_{\mathbf{k}, \sigma} - i\hbar \kappa \sum_{\mathbf{k}, \mathbf{k}'} \left(\hat{a}_{\mathbf{k}'}^{\dagger} \hat{m}_{\mathbf{k}, \mathbf{k}' - \mathbf{k}} - \hat{m}_{\mathbf{k}, \mathbf{k}' - \mathbf{k}}^{\dagger} \hat{a}_{\mathbf{k}'} \right), \quad (1.16)$$

where \mathbf{k} labels the plane-wave modes and $\sigma = 1, 2$ labels the effective spin state for the atoms. The fermionic number and pair operators in momentum space are defined as $\hat{n}_{\mathbf{k}, \sigma} = \hat{c}_{\mathbf{k}, \sigma}^{\dagger} \hat{c}_{\mathbf{k}, \sigma}$ and $\hat{m}_{\mathbf{k}, \mathbf{k}'} = \hat{c}_{\mathbf{k}, 1} \hat{c}_{\mathbf{k}', 2}$, respectively, with $\{\hat{c}_{\mathbf{k}, \sigma}, \hat{c}_{\mathbf{k}', \sigma'}^{\dagger}\} = \delta_{\mathbf{k}, \mathbf{k}'} \delta_{\sigma, \sigma'}$ (while $[\hat{a}_{\mathbf{k}}, \hat{a}_{\mathbf{k}'}^{\dagger}] = \delta_{\mathbf{k}, \mathbf{k}'}$). The strength of the atom-molecule coupling is determined by the parameter κ [29]. Note that because of the pairing terms in the Hamiltonian, we must now use a Gaussian basis with nonvanishing anomalous correlations $m_{\mathbf{k}, \mathbf{k}'}$. However, the description is simplified in the case of a uniform molecular gas, for which $\mathbf{k}' \equiv 0$. The necessary (complex) phase-space variables are then $n_{\mathbf{k}} \equiv n_{\mathbf{k}, \sigma}$, $m_{\mathbf{k}} \equiv m_{\mathbf{k}, -\mathbf{k}}$, $m_{\mathbf{k}}^{\dagger} \equiv m_{-\mathbf{k}, \mathbf{k}}^{\dagger}$ for the fermions and the coherent amplitudes α , α^{\dagger} for the bosons. Note that the use of a non-Hermitian basis leads to $m_{\mathbf{k}}^{\dagger} \neq m_{\mathbf{k}}^*$ and $\alpha^{\dagger} \neq \alpha^*$.

The non-uniqueness of the phase-space mapping can be exploited to give stochastic equations with different numerical properties. One specific set of Itô stochastic differential equations is

$$\begin{aligned} \dot{n}_{\mathbf{k}} &= \alpha m_{\mathbf{k}}^{\dagger} + \alpha^{\dagger} m_{\mathbf{k}} + N_0^{-1/2} n_{\mathbf{k}} (m_{\mathbf{k}} \zeta_1^* + m_{\mathbf{k}}^{\dagger} \zeta_2^*), \\ \dot{m}_{\mathbf{k}} &= -2i\delta_{\mathbf{k}} m_{\mathbf{k}} + \alpha (1 - 2n_{\mathbf{k}}) + N_0^{-1/2} (m_{\mathbf{k}}^2 \zeta_1^* - n_{\mathbf{k}}^2 \zeta_2^*), \\ \dot{m}_{\mathbf{k}}^{\dagger} &= 2i\delta_{\mathbf{k}} m_{\mathbf{k}}^{\dagger} + \alpha^{\dagger} (1 - 2n_{\mathbf{k}}) + N_0^{-1/2} (m_{\mathbf{k}}^{+2} \zeta_2^* - n_{\mathbf{k}}^2 \zeta_1^*), \\ \dot{\alpha} &= -\frac{1}{N_0} \sum_{\mathbf{k}} m_{\mathbf{k}} + N_0^{-1/2} \zeta_1, \\ \dot{\alpha}^{\dagger} &= -\frac{1}{N_0} \sum_{\mathbf{k}} m_{\mathbf{k}}^{\dagger} + N_0^{-1/2} \zeta_2. \end{aligned} \quad (1.17)$$

We here use a time scaled with $t_0 = 1/\kappa \sqrt{N_0}$ and have normalised the molecular field to its maximum value possible $\sqrt{N_0}$, where $N_0 \equiv \sum_{\mathbf{k}} \hat{a}^\dagger \hat{a} + \sum_{\mathbf{k}\sigma} \hat{n}_{\mathbf{k},\sigma}$. It is then clear how the noise terms scale with the total number of particles. The stochastic complex Gaussian noises ζ_j ($j = 1, 2$) obey $\langle \zeta_j(\tau) \zeta_{j'}(\tau') \rangle = 0$, $\langle \zeta_j(\tau) \zeta_j^*(\tau') \rangle = \delta_{jj'} \delta(\tau - \tau')$. In practice we convert the equations to Stratonovich form [31] and integrate them with a semi-implicit method.

1.3.2.1. Optimisation by Means of Gauges

The freedom in choosing the stochastic equations for a given Hamiltonian is in practice inexhaustible. For example, one could make the replacements $\zeta_j \rightarrow \tilde{\zeta}_j = \zeta_j c_j$, $\zeta_j^* \rightarrow \tilde{\zeta}_j^* = \zeta_j^*/c_j$. The complex parameters c_j are knobs one can adjust to improve the numerical performance. This is an example of a simple ‘diffusion’ gauge that can increase the simulation time of Eq. (1.17) by up to 50%.

For the Hubbard model of Eq. (1.5) it is possible to rewrite the interaction term as $\hat{b}_\uparrow^\dagger \hat{b}_\uparrow \hat{b}_\downarrow^\dagger \hat{b}_\downarrow = -\hat{b}_\uparrow^\dagger \hat{b}_\downarrow^\dagger \hat{b}_\uparrow \hat{b}_\downarrow \equiv \hat{m}^\dagger \hat{m}$, which allows the use of a different set of mappings and subsequently an expanded set of phase-space variables: $\{\mathbf{n}_\uparrow, \mathbf{n}_\downarrow, \mathbf{m}, \mathbf{m}^\dagger\}$. Although as yet untested, the inclusion of anomalous variables may allow for a more efficient representation when pairing effects are important.

1.4. Validity Issues

We have here made use of phase-space functions that can be treated *exactly* as probability distributions, leading to a mapping of the quantum evolution onto an ensemble of stochastic trajectories. The price of this exact mapping is that the stochastic trajectories explore a domain that cannot be identified with the physical phase space. The unphysical dimensions tend to harbour unstable regions leading to diverging trajectories and large associated sampling error as the evolution progresses. Furthermore, the mapping to a Fokker–Planck equation requires that the distribution function is sufficiently bounded so that certain boundary terms can be neglected. If, after a certain simulation time, the underlying distribution develops low-order polynomial tails, the mapping is no longer guaranteed to be exact and systematic errors may arise beyond this point.

For the simulation of real-time dynamics, the development of boundary terms is associated with clear signatures, such as individual trajectories undergoing large excursions in phase space (‘spiking’) and a dramatic increase in sampling error. An exact replication of quantum dynamics is achieved up until the emergence of such signatures, which indicate the limits of useful simulation time. For the case of imaginary-time evolution, the situation is more subtle. The trajectories may be

stable even down to very low temperatures, at least in the case of the Hubbard model, with no dramatic increase in sampling error. Yet here too, ‘spiking’ behaviour has been observed at the onset of systematic deviations [23], which can also be detected in the violation of some of the Hamiltonian symmetries. As we discussed above, the effect of the systematic errors can be removed in some situations, at the expense of an increased sampling error, and the exact many-body ground-state recovered by a projection onto a symmetric subspace.

1.4.1. Validity Domain

Generally, the Gaussian method works best for weakly interacting systems, i.e. where the deterministic term in the stochastic equations dominates the diffusion term. In the case of strong interactions, the method provides accurate results up to a certain simulation time, as we have explained above. Note that any Hamiltonian with terms which are at most quartic in the fermionic operators can be mapped onto a set of SDEs via the Gaussian representation. This includes, for example, the general electronic structure problem from quantum chemistry [22], or any system with two-body (but not three-body) interactions.

Acknowledgments

We wish to thank our co-workers, in particular Peter Drummond, Matthias Troyer, and Fakher Assaad, for valuable discussions and fruitful collaborations on various aspects of the fermionic methods. We gratefully acknowledge funding from the Australian Research Council, through the ARC Centre of Excellence for Quantum-Atom Optics.

References

- [1] P. A. M. Dirac, Note on exchange phenomena in the Thomas atom, *P. Camb. Philos. Soc.* **26**, 376, (1930).
- [2] E. P. Wigner, On the quantum correction for thermodynamic equilibrium., *Phys. Rev.* **40**, 749, (1932).
- [3] K. Husimi, Some formal properties of the density matrix, *Proc. Phys. Math. Soc. Jpn.* **22**, 264, (1940).
- [4] E. Sudarshan, Equivalence of semiclassical and quantum mechanical descriptions of statistical light beams, *Phys. Rev. Lett.* **10**, 277, (1963).
- [5] R. Glauber, Coherent and incoherent states of the radiation field, *Phys. Rev.* (1963).
- [6] P. D. Drummond and A. D. Hardman, Simulation of quantum effects in Raman-active waveguides, *Europhys. Lett.* **21**, 279, (1993).
- [7] S. Chaturvedi, P. Drummond, and D. Walls, Two photon absorption with coherent and partially coherent driving fields, *J. Phys. A.* **10**, 187, (1977).
- [8] P. D. Drummond and C. W. Gardiner, Generalized P-representations in quantum optics, *J. Phys. A.* **13**, 2353, (1980).
- [9] K. Cahill and R. Glauber, Density operators for fermions, *Phys. Rev. A.* **59**, 1538, (1999).
- [10] G. C. Wick, A. S. Wightman, and E. Wigner, The intrinsic parity of elementary particles, *Phys. Rev.* **88**, 101, (1952).
- [11] B. L. Schumaker and C. M. Caves. A new formalism for two-photon quantum optics. In eds. L. Mandel and E. Wolf, *Proceedings of the 5th Rochester Conference on Coherence and Quantum Optics [Coherence and Quantum Optics V]*, p. 743. Plenum, (1984).
- [12] F. Haake and M. Wilkens, Quasiprobabilities based on squeezed states, *J. Stat. Phys.* **53**, 345, (1988).
- [13] S. Rahav and S. Mukamel, Gaussian phase-space representation of fermion dynamics: Beyond the time-dependent Hartree–Fock approximation, *Phys. Rev. B.* **79**, 165103, (2009).
- [14] J. F. Corney and P. D. Drummond, Gaussian phase-space representations for fermions, *Phys. Rev. B.* **73**, 125112, (2006).
- [15] J. F. Corney and P. D. Drummond, Gaussian operator bases for correlated fermions, *J. Phys. A.* **39**, 269, (2006).
- [16] M. Ögren, K. V. Kheruntsyan, and J. F. Corney, Stochastic simulations of fermionic dynamics with phase-space representations, *Comput. Phys. Commun.* **182**, 1999, (2011).
- [17] J. F. Corney and P. D. Drummond, Gaussian quantum Monte Carlo methods for fermions and bosons, *Phys. Rev. Lett.* **93**, 260401, (2004).
- [18] J. Hubbard, Electron correlations in narrow energy bands, *Proc. Roy. Soc. Lond. Ser. A.* **276**, 238, (1963).
- [19] P. W. Anderson, The resonating valence bond state in La_2CuO_4 and superconductivity, *Science.* **235**, 1196, (1987).
- [20] M. R. Dowling, M. J. Davis, P. D. Drummond, and J. F. Corney, Monte Carlo techniques for real-time quantum dynamics, *J. Comput. Phys.* **220**, 549, (2007).
- [21] S. Sorella and L. Capriotti, Green function Monte Carlo with stochastic reconfigura-

- tion: An effective remedy for the sign problem, *Phys. Rev. B.* **61**, 2599, (2000).
- [22] F. F. Assaad, P. Werner, P. Corboz, E. Gull, and M. Troyer, Symmetry projection schemes for gaussian Monte Carlo methods, *Phys. Rev. B.* **72**, 224518, (2005).
- [23] P. Corboz, M. Troyer, A. Kleine, I. P. McCulloch, U. Schollwock, and F. F. Assaad, Systematic errors in gaussian quantum Monte Carlo and a systematic study of the symmetry projection method, *Phys. Rev. B.* **77**, 085108, (2008).
- [24] T. Aimi and M. Imada, Gaussian-basis Monte Carlo method for numerical study on ground states of itinerant and strongly correlated electron systems, *J. Phys. Soc. Jpn.* **76**, 084709, (2007).
- [25] A. Paramekanti, M. Randeria, and N. Trivedi, High- T_c superconductors: A variational theory of the superconducting state, *Phys. Rev. B.* **70**, 054504, (2004).
- [26] T. A. Maier, M. Jarrell, T. C. Schulthess, P. R. C. Kent, and J. B. White, Systematic study of d -wave superconductivity in the 2d repulsive Hubbard model, *Phys. Rev. Lett.* **95**, 237001, (2005).
- [27] A.-M. S. Tremblay, B. Kyung, and D. Senechal, Pseudogap and high-temperature superconductivity from weak to strong coupling. towards a quantitative theory (review article), *Low Temp. Phys.* **32**, 424, (2006).
- [28] M. Ögren, K. V. Kheruntsyan, and J. F. Corney, First-principles quantum dynamics for fermions: application to molecular dissociation, *Europhys. Lett.* **92**, 36003, (2010).
- [29] M. J. Davis, S. J. Thwaite, M. K. Olsen, and K. V. Kheruntsyan, Pairing mean-field theory for the dynamics of dissociation of molecular bose-einstein condensates, *Phys. Rev. A.* **77**, 023617, (2008).
- [30] R. Friedberg and T. D. Lee, Gap energy and long-range order in the boson-fermion model of superconductivity, *Phys. Rev. B.* **40**, 6745, (1989).
- [31] C. W. Gardiner, *Stochastic Methods*. (Springer-Verlag, Berlin, 2008), fourth edition.